SINGLE–NEUTRON KNOCKOUT REACTIONS ON ^{34,35}Si

J. Enders, D. Bazin, B. A. Brown, T. Glasmacher, P. G. Hansen, V. Maddalena, K. L. Miller, B. M. Sherrill, M. Steiner, and J. A. Tostevin[a],

Experimental studies and theoretical predictions have observed a change of shell structure when going from the valley of β–stability to nuclei with exotic proton to neutron ratios. Thereby the single–particle properties of low–lying states change, as, e. g., expressed in the quantum numbers and spectroscopic factors. Recent investigations [1–6] at the NSCL have proven to determine spectroscopic factors and the orbital angular momenta ℓ of single nucleons reliably from fast exotic ion beams ($E_{\rm kin} \geq 50\,A$ MeV). In these experiments, one observes the projectile residues from single–nucleon removal reactions in inverse kinematics in the high–resolution S800 spectrograph. Different final states populated in the reaction can be disentangled by measuring their γ decay with a position–sensitive NaI(Tl) detector array [7]. For an overview over the theoretical description of the reaction process, see [8, 9] and references therein.

Previous studies have focused on nuclei in the proton and neutron 0*p* and 1*s*0*d* shells. The experiment described here probes single–particle properties in the neutron–rich Si isotopes at the $N = 20$ shell closure. It was hoped to detect the signature of an $\ell = 3$ neutron removal from ^{35}Si for the first time. It also serves as a test of the applicability of the particle removal reaction in this mass region where (a) intruder configurations play an important role and (b) the level density of bound final states is much higher than in previous experiments. Additionally, one can look for the influence of spin–orbit forces on the momentum distributions that is predicted by some theoretical approaches [10].

Radioactive ^{34,35}Si beams were produced from fragmentation of a 100 A MeV ^{40}Ar beam and analyzed in the A1200 fragment separator. The secondary beams with energies of $\sim$ 74 A MeV impinged on a 0.5 mm thick ^{9}Be target that was surrounded by an array of position–sensitive NaI(Tl) detectors [7]. The reaction residues were momentum analyzed in the S800 spectrograph operating in dispersion–matched mode. We refer to [5] for further details of this type of experiment. Data were taken for 6 hours in the case of ^{34}Si (incident secondary particle rate $\sim 2\,200$ s^{-1}) and for about 34 hours in the case of the ^{35}Si neutron–removal reaction (~ 260 s^{-1}).

After identification of the reaction residues in the S800 focal plane, the inclusive cross sections could be determined. They contain contributions from both the stripping (i. e., the removed neutron is absorbed in the target) and the diffraction process (the removed neutron is scattered).

In order to disentangle the contributions from different final states, the γ–ray spectra in coincidence with the reaction residues need to be analyzed. Figure 1 shows the extracted photon spectra after reconstruction of the center–of–mass energy of the emitted photon, i. e., correcting for the Doppler effect. The histogram in the upper part of the figure displays the experimental results for the neutron knockout from ^{34}Si, the lower part shows the result for the neutron removal from ^{35}Si. One observes broad peak structures — due to the limited resolution of the NaI(Tl) detectors and the Doppler effect — residing on a continuous "background". Previous experiments (see [11] for a discussion) are in rough agreement with the continuous distribution observed in the (^{34}Si,^{33}Si) reaction, which appears to be the simpler of the two spectra shown in Fig. 1. We therefore parametrized the shape of the background distribution from a fit to the (^{34}Si,^{33}Si+γ) spectrum by a single exponential function. This shape was also used to describe the continuous distribution in the neutron knockout from ^{35}Si.

The γ–ray spectrum of the (^{35}Si,^{34}Si+γ) reaction is rather complex because many states below the neutron threshold in the residue ^{34}Si are to be populated. This is expected from the shell model, and various excited states in the residue ^{34}Si have been observed recently in a β–decay experiment [12]. The experimental photon spectrum can be described rather well if one assumes the continuous background from the ^{34}Si neutron–removal reaction also for the ^{35}Si neutron knockout and fits the line shapes of transitions known from β decay [12] to it. To obtain a line shape, simulations with the code GEANT [13] are used which include both the Lorentz boost as well as the reconstruction of the center–of–mass energy from the detector signals. The dotted lines in

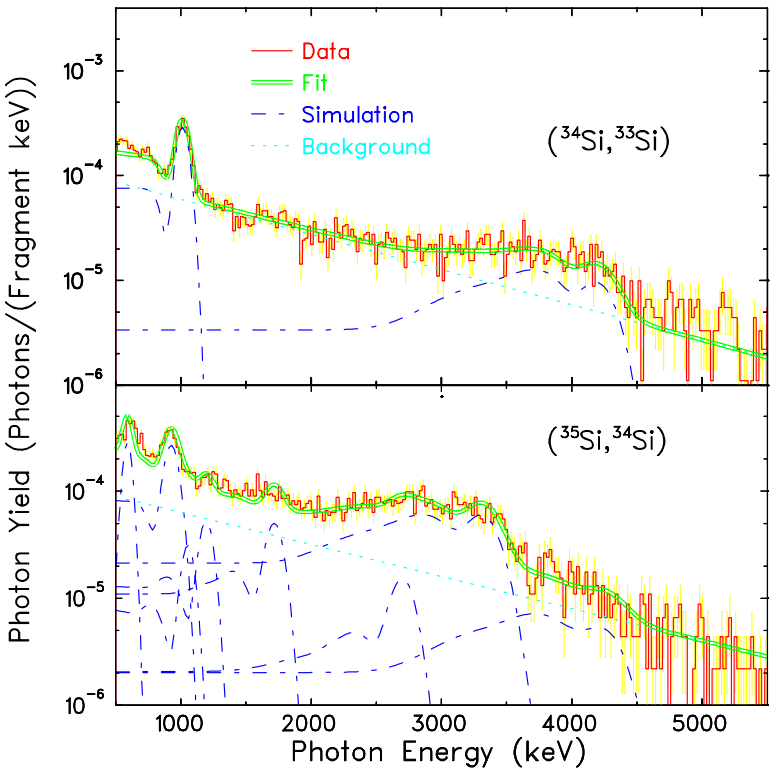

Figure 1: Photon spectra measured in coincidence with the single–neutron knockout from ^{34}Si (top) and ^{35}Si (bootom). The histogram shows the experimental data. The dotted line shows the continuous background distribution. The dash–dotted curves show the line shapes of transitions, taking the Doppler shift as well as the reconstruction process into account. The double solid line displays the fit of the line shapes and the continuous distribution to the experimental data.

Fig. 1 show the continuous distribution in the two measurements along with the line shapes (dash–dotted lines) fitted to the measured spectrum. The agreement between the sum of all components (double solid line) and the data (histogram) is generally good. The energies of excited states deduced from the photon spectrum of the (^{34}Si,^{33}Si+γ) reaction agree well with the results of a previous Coulomb excitation experiment [14].

By normalizing the simulated line shapes to the measured data, it is possible to extract the cross sections for the population of specific final states. These are given in Tab. 1 both for (^{34}Si,^{33}Si) and (^{35}Si,^{34}Si). The results given are up to now preliminary because corrections taking the S800 acceptance into account still need to be included.

For comparison with the experimental results, Tab. 1 also lists the total angular momenta and parities J^π of the populated final states and the orbital and total angular momenta $N\ell j$ of the removed particle, both as predicted from the shell model. The cross section expected from theory $\sigma^{\rm Th}$ contains the spectroscopic factors C^2S, calculated within the shell model, and the single–particle removal cross section, which was obtained from the reaction model described in Refs. [8,9]. The experiment observes a somewhat stronger population of the g. s. than predicted by theory; for all other cases, the agreement between theory and experiment is rather good.

As is evident from the lower part of Fig. 1, it is not possible to extract further information from applying gates to the γ–ray spectrum for the removal reaction on ^{35}Si due to the complexity of the spectrum. Applying such gates in the case of the (^{34}Si,^{33}Si) reaction leads to the parallel momentum distributions displayed in Fig. 2 for the ground state, the excited state at about 1 MeV, and the excited state at about 4 MeV, respectively. The data are shown as full points and compared to calculations using the Eikonal approximation according to Ref. [15]. While in the earlier calculation, valid for halo states, the wave function was approximated by its value along the

Table 1: Exclusive single–neutron removal cross sections (preliminary). Given are the excitation energy in the residual nucleus $E_{\mathrm{x},f}$, the total angular momentum and parity of the final state J^π_f, the major quantum number, orbital and total angular momentum $N\ell j$ of the removed particle (as predicted from the shell model), the spectroscopic factor C^2S as calculated within the shell model, the theoretical cross section σ_f^{Th} and the measured cross section σ_f^{Exp}. Final states marked with an asterisk have not been detected in the experiment or cannot be placed clearly in the level scheme. The J^π_f values in parentheses are suggested by theory.

^{34}Si to ^{33}Si @ 73.4 A MeV; $S(n) = 7.36$ MeV					
$E_{\mathrm{x},f}$ (MeV)	J^π_f ($\hbar$)	$N\ell j$ ($\hbar$)	C^2S	σ_f^{Th} (mb)	σ_f^{Exp} (mb)
0.00	$(3/2)^+$	$0d_{3/2}$	3.56	53	65(9)
1.01	$(1/2)^+$	$1s_{1/2}$	1.46	30	41(5)
4.20	$(5/2)^+$	$0d_{5/2}$	2.50	29	15(3)
4.32*	$(3/2)^+$	$0d_{3/2}$	0.11	$\sim$1	—
4.93*	$(1/2)^+$	$1s_{1/2}$	0.42	$\sim$7	$<$2
5.68*	$(5/2)^+$	$0d_{5/2}$	0.76	$\sim$8	—
Σ				~ 128	121(14)

^{35}Si to ^{34}Si @ 73.8 A MeV; $S(n) = 2.75$ MeV					
$E_{\mathrm{x},f}$ (MeV)	J^π_f ($\hbar$)	$N\ell j$ ($\hbar$)	C^2S	σ_f^{Th} (mb)	σ_f^{Exp} (mb)
0.00	0^+_1	$0f_{7/2}$	0.86	18	33(9)
2.13	0^+_2	coll.	—		
3.33	2^+_1	coll.	—	0	12(8)
4.26	3^-_1	$0d_{3/2}$	0.63	10	28(8)
	3^-_1	$1s_{1/2}$	0.11	3	
4.38	(4^-_1)	$0d_{3/2}$	0.94	14	
4.97	(5^-)	$0d_{3/2}$	1.19	17	11(6)
5.04*	(2^-)	$0d_{3/2}$	0.47	7	13(5)
	(3^-)	$1s_{1/2}$	0.55	12	
6.02*	(3^-)	$0d_{3/2}$	0.0	0	10(5)
	(4^-)	$1s_{1/2}$	0.77	15	
Σ				$\sim$96	106(19)

axis of the target trajectory, the present work (and also [1–5]) used the full three–dimensional integration. The theoretical distributions have been scaled to match the data.

For the momentum distributions associated with the population of the excited states with tentative quantum numbers $J^\pi = (1/2^+)$ and $J^\pi = (5/2^+)$ the shapes of an *s*– and a *d*–wave removal are clearly visible. The detected low–momentum tail of the *s*–wave knockout is in agreement with the coupled discretized continuum channel approach of Ref. [9], and it reflects energy conservation in the diffractive channel. For the momentum distribution in coincidence with the population of the g. s. one finds, however, that the deduced shape is in conflict with the simple calculations for both the *s*– and the *d*–wave knockout. In addition, the centroid of the distribution appears to be shifted to smaller momenta. This behavior is up to now still not understood but could be a real effect. (This is the first $d_{3/2}$ momentum distribution measured in our experiments.) Additional data analysis work is in progress. A possible explanation might be the appearence of spin–orbit effects leading to a forward–backward asymmetry. Such effects are predicted within the transfer to the continuum model of Ref. [10], but prelimiary calculations [16] do not match the experimental data.

We acknowledge helpful discussions with A. Bonaccorso and financial support by the U. S. National Science Foundation, contract numbers PHY–00 70911 and PHY–95 28844.

a: Department of Physics, University of Surrey, Guildford, Surrey, United Kingdom

References

1. A. Navin *et al.*, Phys. Rev. Lett. **81**, 5089 (1998)
2. T. Aumann *et al.*, Phys. Rev. Lett. **84**, 35 (2000)
3. V. Guimarães *et al.*, Phys. Rev. C **61**, 064609 (2000)
4. A. Navin *et al.*, Phys. Rev. Lett. **85**, 266 (2000)
5. V. Maddalena *et al.*, Phys. Rev. C **63**, 024613 (2001)
6. P. G. Hansen, B. M. Sherrill, Nucl. Phys. A, in press

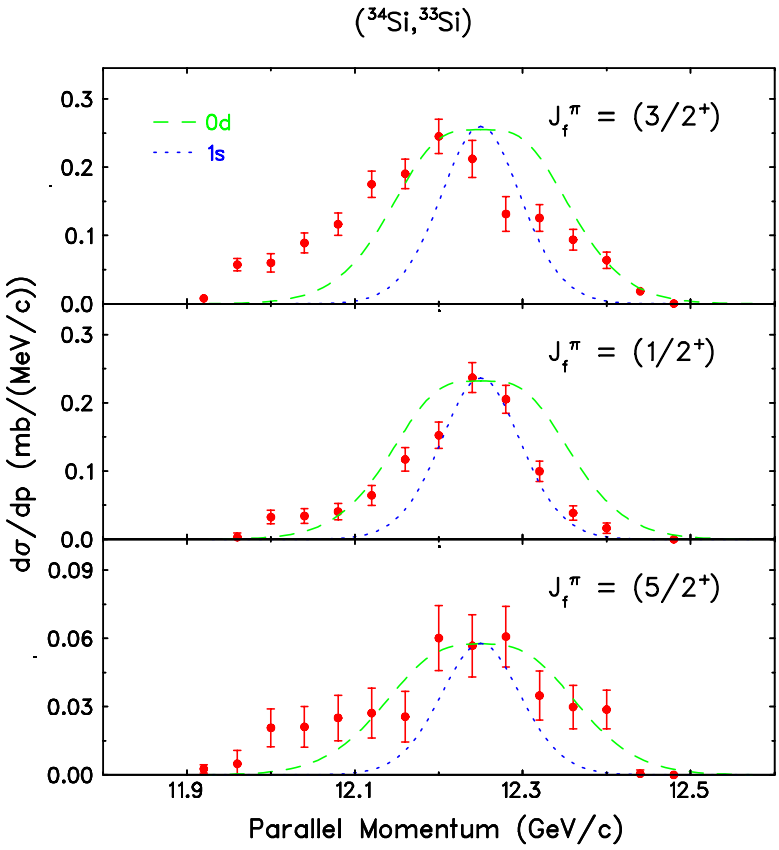

Figure 2: Parallel momentum distributions for the (^{34}Si,^{33}Si+γ) reaction, gated on the γ rays depopulating the states at 1.01 MeV (middle) and at 4.20 MeV (bottom). The top part shows the momentum distribution for the reaction channel into the ground state of ^{33}Si. The experimental data are shown as full points. The dotted and dashed lines are calculated from the Eikonal approach of Ref. [15] for *s*– and *d*–wave removal, respectively. The theoretical curves are scaled to the data, while the absolute values are discussed in Tab. 1.

7. H. Scheit, T. Glasmacher, R. W. Ibbotson, P. G. Thirolf, Nucl. Instr. Meth. in Phys. Res. A **422**, 124 (1999)
8. J. A. Tostevin, J. Phys. G **25**, 735 (1999)
9. J. A. Tostevin, Nucl. Phys. A **682**, 320c (2001)
10. A. Bonaccorso, Phys. Rev. C **60**, 054604 (1999)
11. V. Maddalena, Ph. D. Thesis, Michigan State University (2000)
12. S. Nummela *et al.*, Phys. Rev. C **63**, 044316 (2001)
13. GEANT, Version 3.21, CERN Program Library Long Writeup W5013, Geneva (1994)
14. B. V. Pritychenko *et al.*, Phys. Rev. C **62**, 051601(R) (2000)
15. P. G. Hansen, Phys. Rev. Lett. **77**, 1016 (1996)
16. A. Bonaccorso, private communication (2000)